UDC 621.314
DOI: 10.18799/24131830/2025/5/4857
Review article

Advantages of using transformers with high temperature superconducting windings at high frequency in mobile and autonomous power supply systems

R.G. Galeev[1]✉, V.Z. Manusov[2], E.N. Larkin[3]

[1] Novosibirsk State Technical University, Novosibirsk, Russian Federation
[2] Yugra State University, Khanty-Mansiysk, Russian Federation
[3] Siberian State University of Water Transport, Russian Federation

✉galeew.ratmir@yandex.ru

Abstract. ***Relevance.*** Active and passive elements of transformer power equipment have sufficiently reduced the potential for modernization and improvement that requires new innovative solutions. This largely relates to mobile and autonomous power supply systems, in particular for geoengineering tasks when changing the location of geo-surveying works. ***Aim.*** New design of transformer power equipment based on cryogenic technologies with improvement of their electrical, technical and economic characteristics involves the use of liquid nitrogen with a temperature of 77 K as a cryogenic dielectric medium. ***Methods.*** Mathematical modeling of the skin-effect by a finite-element method, determination of the amorphous alloy magnetic core characteristic by an empirical method, and physical simulation of an experimental model for a high temperature superconducting transformer prototype. ***Results and conclusions.*** The paper introduces the analysis and synthesis of characteristics of amorphous iron magnetic core and superconducting windings in a high temperature superconducting transformer. The authors have derived dependencies and charts illustrating the effect of increased current frequency on thermal losses associated with hysteresis and eddy currents, which determine the losses in the magnetic core. The paper demonstrates the dependence of mass and dimensions reduction and winding material consumption on frequency and current density in high temperature superconducting tapes, which can reach 500 A/mm^2. This affects in its turn the size of transformer windings and, therefore, the size of the magnetic core. The most significant result with the use of superconductivity in high temperature superconducting transformers is the fact that this transformer is an ideal diamagnetic, and the windings have high electrical conductivity. Therefore, the problem of current concentration near the conductor surface skin-effect and resistance increase is eliminated in transformers and electric machines. The absence of skin-effect in high temperature superconducting conductors due to zero resistance is proved by the theoretical analysis using Bessel functions. The importance of the results involves the increase of transformer efficiency at higher frequencies due to the synthesis of properties of transformer active elements, such as amorphous iron magnetic core, high temperature superconducting windings and liquid nitrogen as a dielectric medium. On this basis, a 25 kVA high temperature superconducting transformer industrial prototype was designed and assembled.

Keywords: skin-effect, superconductivity, high frequency, amorphous magnetic core, HTS transformer, liquid nitrogen

For citation: Galeev R.G., Manusov V.Z., Larkin E.N. Advantages of using transformers with high temperature superconducting windings at high frequency in mobile and autonomous power supply systems. *Bulletin of the Tomsk Polytechnic University. Geo Assets Engineering*, 2025, vol. 336, no. 5, pp. 183–194. DOI: 10.18799/24131830/2025/5/4857

УДК 621.314
DOI: 10.18799/24131830/2025/5/4857
Шифр специальности ВАК: 2.4.3
Обзорная статья

Преимущества использования трансформаторов с высокотемпературными сверхпроводящими обмотками на повышенной частоте в мобильных и автономных системах электроснабжения

Р.Г. Галеев[1]✉, В.З. Манусов[2], Е.Н. Ларкин[3]

[1] Новосибирский государственный технический, Россия, г. Новосибирск
[2] Югорский государственный университет, Россия, г. Ханты-Мансийск
[3] Сибирский государственный университет водного транспорта, Россия, г. Новосибирск

✉galeew.ratmir@yandex.ru

Аннотация. ***Актуальность***. Активные и пассивные элементы трансформаторного электрооборудования достигли своего предела совершенства, что существенно ограничивает возможности для дальнейшей модернизации и требует разработки новых инновационных решений. Это в значительной степени относится к мобильным и автономным системам электроснабжения, в частности для решения задач геоинжиниринга при изменении локации геоизыскательных работ. ***Цель.*** Новое конструктивное исполнение трансформаторного электрооборудования на основе криогенных технологий с улучшением их электрических и технико-экономических характеристик, где в качестве криогенной диэлектрической среды используется жидкий азот при температуре 77 К. ***Методы.*** Математическое моделирование явления скин-эффект методом конечных элементов; определение характеристики магнитопровода из аморфного сплава эмпирическим методом и физическое моделирование экспериментальной модели прототипа высокотемпературного сверхпроводящего трансформатора. ***Результаты и выводы.*** Приведен анализ и синтез характеристик магнитопровода из аморфного железа и сверхпроводящих обмоток в высокотемпературном сверхпроводящем трансформаторе. Получены зависимости и графики влияния повышения частоты тока на тепловые потери, связанные с гистерезисом и вихревыми токами, из которых складываются потери в магнитопроводе, а также показана зависимость уменьшения массы сердечника и витков обмоток от частоты с использованием высокотемпературной сверхпроводящей ленты, в которой плотность тока может достигать 500 А/мм^2. Это в свою очередь влияет на размеры обмоток трансформатора и, следовательно, на размеры магнитопровода. Наиболее существенным результатом с использованием явления сверхпроводимости в высокотемпературных сверхпроводящих трансформаторах является тот факт, что они являются идеальным диамагнетиками, а обмотки имеют высокую величину электрической проводимости, следовательно, в трансформаторах и электрических машинах исчезает проблема вытеснения тока к поверхности проводника – «скин-эффект» и увеличения сопротивления. С помощью теоретического анализа с использованием условий функций Бесселя доказано отсутствие скин-эффекта в высокотемпературных сверхпроводящих проводниках по причине нулевого активного сопротивления. Значимость результатов заключается в повышении КПД трансформатора при работе на повышенных частотах благодаря синтезу свойств активных элементов трансформатора: магнитопровода из аморфного железа, высокотемпературных сверхпроводящих обмоток и диэлектрической среды из жидкого азота. На этой основе разработан и создан промышленный экземпляр высокотемпературного сверхпроводящего трансформатора мощностью 25 кВА.

Ключевые слова: скин-эффект, сверхпроводимость, повышенная частота, аморфный магнитопровод, ВТСП трансформатор, жидкий азот

Для цитирования: Галеев Р.Г., Манусов В.З., Ларкин Е.Н. Преимущества использования трансформаторов с высокотемпературными сверхпроводящими обмотками на повышенной частоте в мобильных и автономных системах электроснабжения // Известия Томского политехнического университета. Инжиниринг георесурсов. – 2025. – Т. 336. – № 5. – С. – 183–194. DOI: 10.18799/24131830/2025/5/4857

Introduction

When designing autonomous and mobile power supply systems and conducting geological survey expeditions, the issue of energy efficiency and mass and dimensional parameters of transformer power equipment and energy storages is urgent. The use of semiconductor voltage converters, which can replace power transformers operated on the physical

phenomenon of electromagnetic induction, is a promising direction of power engineering development. However, semiconductor devices are very expensive equipment at the moment and also very unreliable that can lead to power supply failures and even accidents under specific circumstances. The priority device for voltage transformation at a given frequency is transformer power equipment based on magnetically coupled inductive coils (inductors).

A transformer, being a highly reliable device of simple construction, has a low specific power per unit mass, approximately 180 W/kg. Taking into account that transformer power equipment is included in the mobile power supply system, its energy efficiency and mass and dimensions parameters have a great effect on the ability of mobile objects to move during geological explorations, in particular in the northern regions of Russia, including the Polar (Arctic) Circle. The use of an increased frequency of the generation source, an amorphous magnetic core and superconducting in the complex will significantly reduce the weight and size characteristics and increase efficiency of transformers.

Earlier, a practical investigation of a high-frequency pulse power transformer with a mixed core at 200 kHz was carried out 1. The author concluded that the combination of core layers of amorphous, ferrite and electrical iron resulted in a decrease in the hot spot temperature that increased the rated power of the transformer. The numerical simulation of the skin-effect (SE) is performed in 2 with the determination of its influence on the reactance and comparison with experimental measurements of copper wires at $0.1 \cdot 10^4$ kHz. The paper [3] describes the anisotropy of the critical current in a superconducting air-core transformer at 2.2 kHz. The impact of cryogenic environment on the characteristics of electrical and amorphous iron magnetic cores is shown in [4, 5].

Aim. New design of transformer power equipment based on cryogenic technologies with improvement of their electrical, technical and economic characteristics involves the use of liquid nitrogen with a temperature of 77 K as a cryogenic dielectric medium.

In practice, several methods are used to reduce the mass-dimensional parameters of transformer power equipment, namely:

- application of magnetic core material with high magnetic characteristics at an increase in frequency up to 800 Hz;
- application of materials with high current density for transformer windings;
- increase of the operating frequency in the electrical system.

Basic background

At present, most transformer magnetic cores are made of electrical steels and ferrites. The maximum operating induction, at which a transformer has acceptable magnetic core losses within the technical specifications, is in the range of B_c=1.6–2 T. Reduction of transformer dimensions by increasing the current density is a promising direction due to the development of high temperature superconducting (HTS) wires of the 2nd generation [6–9].

The design of transformer windings from a superconducting wire, which has zero AC resistance at the boiling temperature of liquid nitrogen 77 K/–198 °C, allows eliminating resistance losses [5]. The current density in a superconducting wire can reach 500 A/mm^2, in comparison with 2.8 A/mm^2 for copper. The difference of 250 times has a significant role in reducing the volume and weight of transformer windings [10–13].

The most effective method to reduce the dimensions and weight of the transformer is related to the increase of the operating current frequency (1), but requires a careful approach to the selection of applied materials and transformer design [14–16]:

$$d = 0{,}507 \sqrt[4]{\frac{P' \beta a_r k_r}{f u_r B^2 K_c^2}}, \quad (1)$$

where P' is the single-phase power; $\beta=\pi d/l$ is the value determining the ratio between the diameter (d) and the height (l) of the winding; a_r is the effective width of the dissipation field; k_r is the coefficient of reducing the ideal dissipation field to the actual one (Rogowski coefficient); f is the network frequency, Hz; u_r is the reactive component of the short circuit voltage, %; B is the maximum induction in the core leg; k_c is the coefficient of filling the circle area with steel.

As follows from (1), the AC frequency and the core diameter are inversely proportional. Consequently, the magnetic core weight of a superconducting transformer is significantly reduced. When increasing the frequency, the number of turns of the transformer windings decreases (2). It should be noted that when the winding diameter decreases, the distance between the core legs also decreases. This results in a reduction of the window area of the magnetic core. Consequently, the volume and weight of the core iron decreases.

$$W = \frac{U}{4{,}44 f B S}, \quad (2)$$

where U is the voltage; S is the active electrical steel area of the magnetic core.

Mathematical models and analysis of the SE for transformer operation at high frequency

The use of high frequencies always results in the current concentration near the outer part of the conductor, which was called the SE [17–19].

At the industrial frequency of 50 or 60 Hz used in the world practice, the resistance to the SE is negligible and is not usually taken into account. The effect is

caused by the presence of the magnetic flux in the internal part of the conductor, which is induced by the operating current in the wire. The current induced by the internal magnetic flux has an opposite direction to the operating current I when being closer to the center of the wire, and has the same direction for the outer part of the conductor. The SE results in the exponential decrease of the current density with the depth.

The non-uniform current distribution along the cross section of the conductor can be clarified by theoretical analysis using Bessel functions, which consider the presence of internal induction in the conductor being several orders of magnitude less than the external induction. For complex amplitudes of the current density and the magnetic field strength, equations (3), (4) are applied:

$$\frac{d^2 J_m}{dr^2} + \frac{1}{r}\frac{dJ_m}{dr} = j\omega\mu\sigma J_m, \quad (3)$$

$$\frac{d^2 \dot{H}_m}{dr^2} + \frac{1}{r}\frac{d\dot{H}_m}{dr} - \frac{\dot{H}_m}{r^2} = j\omega\mu\sigma\dot{H}_m, \quad (4)$$

where J_m is the complex amplitude of the current density; $\dot{H}_m$ is the magnetic field strength; r is the resistance; σ is the conductivity of the conductor; μ is the magnetic permeability; ω is the angular frequency.

The impedance of a cylindrical conductor is determined by the sum of the internal impedance and the external impedance of the conductor (5), (6):

$$Z = Z_{\text{in}} + Z_{ext}. \quad (5)$$

The internal impedance is defined by equation (6):

$$Z_{in} = R_{dc} \cdot \frac{u_a}{2}\frac{J_0(u_a)}{J_1(u_a)} = Re(Z_{in}) + I_m(Z_{in}), \quad (6)$$

where R_{dc} is the DC resistance of the conductor under steady-state conditions; $J_0(u_a)$ and $J_1(u_a)$ are the Bessel functions of the zero and first order, respectively; $u_a = j^{2/3}\sqrt{2x}$, $x=a/\delta$, a is the conductor radius; δ is the surface layer depth; $Re(Z_{in})$ is the real component of the internal impedance; $I_m(Z_{in})$ is the complex inductive component of the internal impedance.

The external impedance is defined by equation (7):

$$Z_{ext} = jX_{ext} = j2\pi f L_{ext}. \quad (7)$$

The series decomposition of the Bessel function is given by (8):

$$\frac{u_a}{2}\frac{J_0(u_a)}{J_1(u_a)} = 1 - \frac{u_a^2}{8} - \frac{u_a^4}{192} - \frac{u_a^6}{3074} - \ldots \quad (8)$$

The electromagnetic surface depth δ (9), at which the current density is $1/e$ (≈37%) of its surface density, is determined by the equation [17]:

$$\delta = \sqrt{\frac{1}{\pi\sigma f \mu}}, \quad (9)$$

where σ is the conductivity of the conductor; μ is the permeability of the conductor.

From the surface to the center of the conductor, the current density J decreases according to the exponential dependence (10):

$$J_Z = J_0 \cdot e^{-\frac{z}{\delta}}, \quad (10)$$

where J_0 is the current density at the surface; z is the depth of the calculation.

It follows from (6) and (7) that the closer to the center of the conductor, the lower the current density. Thus, a considerable area of the wire cross-section is not involved in the electricity transmission (Fig. 1).

The above analysis shows that it is necessary to take into account the SE when designing a superconducting transformer operated at high frequencies. Using ELCUT software (professional version 6.6) [20], the simulation of current concentration near the surface was carried out by a finite-element method for a copper conductor of 5.7 mm diameter and 2.4 A/mm^2 current density at AC frequencies of 200, 400 and 800 Hz.

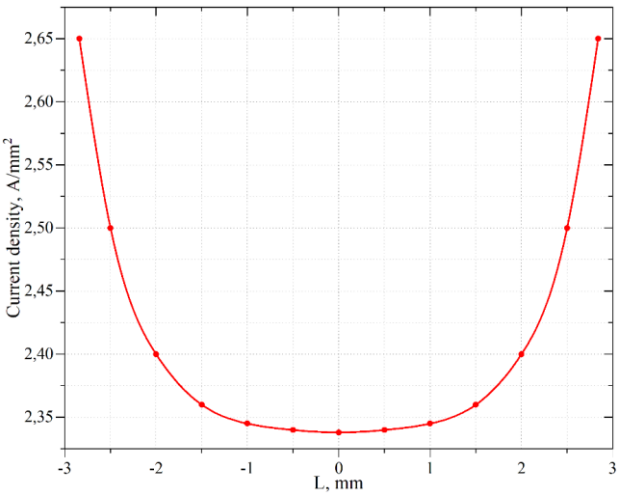

Fig. 1. *Current density change along the conductor cross section*

Рис. 1. *Изменение плотности тока по поперечному сечению проводника*

Fig. 2 shows a color diagram of the current concentration near the conductor surface (SE illustration). A finite element mesh with 1306 nodes was obtained in the cross section of the 25.5 mm^2 copper conductor with a sampling step of 0.05 mm. This fully illustrates the phenomenon when the SE becomes more evident at 400 Hz and above. Copper is

diamagnetic in its magnetic properties, but its magnetic permeability is greater than zero being equal to μ=0.999990. This results in the magnetic field penetration into the conductor depth and the formation of magnetic induction of a certain strength leading to the appearance of eddy currents. The increase of eddy currents, in its turn, causes more intensive current forcing to the conductor surface. In this regard, the rise of heat generation and voltage drop are observed.

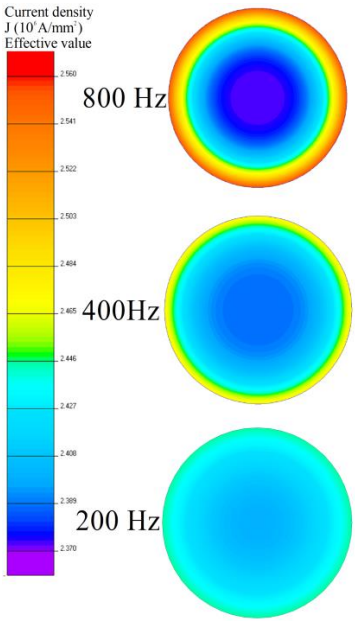

Fig. 2. *Color diagram of the SE when forcing the current to the conductor surface with the frequency increase*
Рис. 2. *Цветовая диаграмма скин-эффекта тока к поверхности проводника с увеличением частоты*

Superconductors are absolute diamagnetics, which magnetic permeability is zero. This means that the magnetic field is completely eliminated from the conductor volume under the superconducting state. In a superconductor, electrons form pairs called Cooper pairs, thus providing the superconducting state. They have zero spin and can move without interaction with the crystal lattice, causing zero resistance in the material. This is confirmed by the effect of expelling the external magnetic field from the superconductor body due to internal eddy currents (Meissner effect) in superconductors. HTS conductors have zero resistance at 77 K, hence it is difficult to apply equation (9).

Investigation of HTS transformers at high frequencies

For investigating the properties and characteristics of the transformer magnetic core made of the soft magnetic fast-quenched 1CP amorphous alloy with the 1B AMET magnetic core were analyzed at different network frequencies [21].

Fig. 3 shows the hysteresis loop of the amorphous core obtained experimentally using an oscilloscope. The rectangular shape of the loop is a feature of amorphous alloys, due to which the value of coercive force corresponds to the operating value of magnetic field strength.

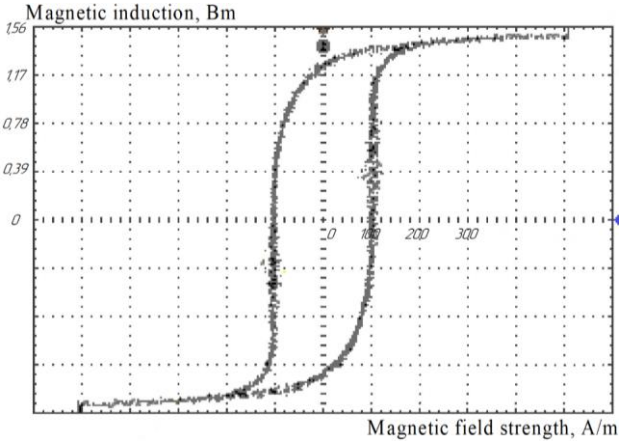

Fig. 3. *Magnetic characteristic of the 1B AMET magnetic core*
Рис. 3. *Магнитная характеристика магнитопровода 1 В AMET*

The 1CP tape has the following alloying elements: B, Si, P, C, Co, Ba. Obtained by quenching from the liquid state due to high cooling rate (>1000 K/s), the metal passes into the passive state that provides high corrosion resistance for various aggressive media. These properties of amorphous alloys make them an excellent analog of conventional electrical steel for designing power transformers with high energy efficiency [22, 23].

Table 1 shows the technical characteristics of the HTS transformer.

The investigation is particularly focused on the relationship between the transformer core remagnetization frequency and the change of the magnetic core dimensions, hysteresis loop losses and eddy current losses.

The remagnetization losses and eddy current losses are calculated according to the Steinmetz equation [16]:

$$P_h = nfB^2G_{st}, \quad (11)$$

$$P_{ed} = yf^2B^2G_{st}, \quad (12)$$

where y and n are the coefficients characterizing the used ferrimagnetic material; G_{st} is the transformer core weight.

The coefficients n and y were determined from the parameters of the hysteresis loop area to the magnetic core volume at 50 Hz (Fig. 3) and specific losses in the 1B amorphous alloy.

Table 1. *Initial technical characteristics of the HTS transformer*

Таблица 1. *Параметры сверхпроводящего трансформатора*

Parameter/Параметр	Value/Величина	
Rated power, kVA Номинальная мощность, kVA	100	
Number of phases/Ччисло фаз	3	
Winding connection Соединение обмоток	△/Yn-0	
Cryostat material Материал криостата	Expanded polystyrene Пенополистирол	
Dielectric medium Диэлектрическая среда	Liquid nitrogen Жидкий азот	
Operating temperature, K Температура жидкой фазы, K	77	
Current frequency, Hz/Частота, Гц	50, 200, 400, 800	
Winding parameters/Параметры обмоток		
Type of winding Тип обмотки	HV winding Обмотка ВН	LV winding Обмотка НН
Rated voltage, V Номинальное напряжение, В	10000	400
HTS tape width (ширина высокотемпературной сверхпроводящей ленты, мм), mm	4×0,1	12×0,1
Insulation Изоляция	Polyamide varnish Полиамидный лак	
Rated current/Номинальный ток, A	3.7	162.5
Current density, A/mm² Плотность тока, А/мм²	9.25	135
Magnetic core parameters/Параметры магнитной системы		
Material Материал	Amorphous magnetic core 1B Аморфный магнитопровод	
Alloying elements Легирующие элементы	B, Si, P, C, Co, Ba	
Saturation induction, Bm Индукция насыщении, Bm	1,57	

The obtained dependences of the magnetic core losses with the frequency increase are shown in Fig. 4.

According to Steinmetz equation (11), (12) and Fig. 4, there is a linear dependence of hysteresis losses and an exponential dependence of eddy current losses on the frequency increase. Modern electrical steels have relatively high magnetic saturation induction up to 2 T [24], but low magnetic permeability that, in its turn, leads to a considerable increase in the magnetic field strength to achieve the required induction in the core. This results in an enlarged area of the hysteresis loop that illustrates remagnetization losses.

To reduce the losses in the magnetic core associated with the core remagnetization, it is reasonable to use amorphous alloys. Such alloys lack strict periodicity and long-range order in the arrangement of atoms that is inherent in the crystal structure of magnetically soft electrical steels, which do not have inter-domain boundaries, as shown in Fig. 5. Due to high values of magnetic permeability (μ=50000–70000), amorphous alloys are preferably used in power transformers at high frequencies [25].

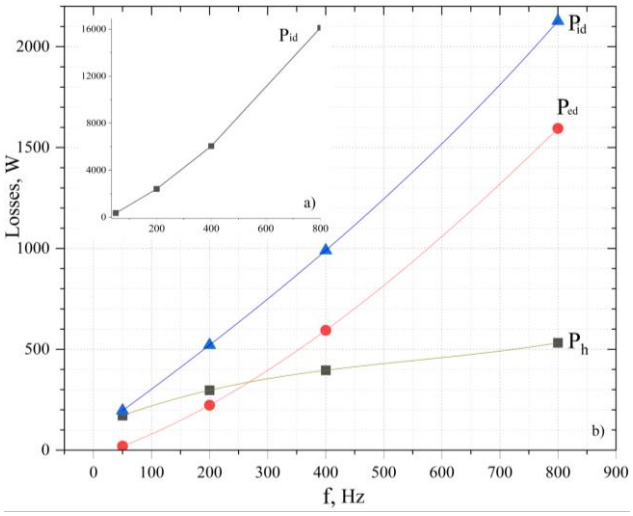

Fig. 4. *Dependences of hysteresis losses and eddy current losses: a) electrical steel of 3408 grade: P_{id} are the losses in the magnetic circuit b) 1B amorphous magnetic core: P_{id} are the losses in the magnetic circuit; P_{ed} are the eddy current losses; P_h are the hysteresis losses*

Рис. 4. *Потери в магнитопроводе при повышении частоты: а) электротехническая сталь 3408: P_{id} – полные потери в магнитопроводе; b) Аморфный магнитопровод марки 1В: P_{ed} – потери на вихревые токи; P_h – потери на гистерезис*

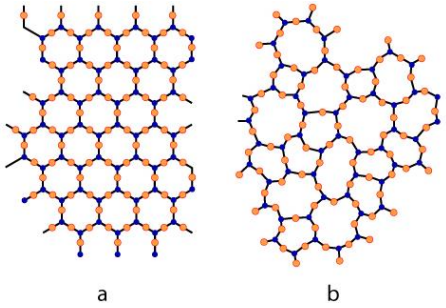

Fig. 5. *Atoms of: a) crystal; b) amorphous structure*

Рис. 5. *Расположение атомов: а) кристаллической и b) аморфной структуры*

For modern electrical steel used in a transformer, with plate thicknesses of 0.17–0.5 mm and depending on the magnetic core design, the ratio P_B/P_h can vary in the range of 0.2–7. In the case of amorphous iron, the ratio P_B/P_h is in the range of 0.17–2.9 at high network frequencies of 50–800 Hz. This is due to the high resistivity of 100–300 μOhm·cm, which is slightly higher than the resistance of cold-rolled steel being in the range of 40–80 μOhm·cm [26, 27].

The next important point is to reduce the core volume, hence its weight according to (1). The dependence f and the magnetic core weight are inversely proportional as presented in Fig. 6.

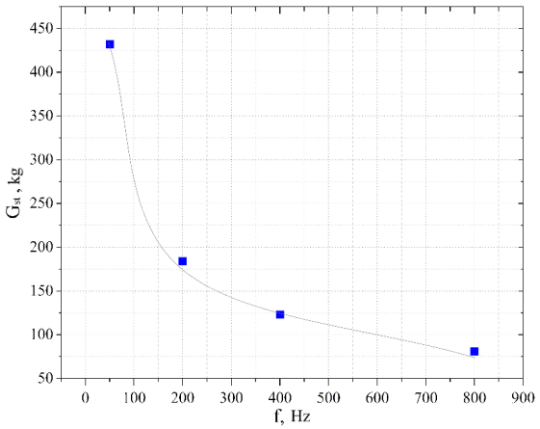

Fig. 6. *Dependence between the remagnetization frequency and the core weight*
Рис. 6. *Зависимость массы сердечника от частоты*

In the paper, the dependence illustrating the effect of increasing frequency on the EMF (13) growth was obtained that directly affects the number of turns of transformer windings (Fig. 7). The found characteristics of the HTS transformer at the frequency increase are summarized in Table 2.

$$E = 4,44fBS. \quad (13)$$

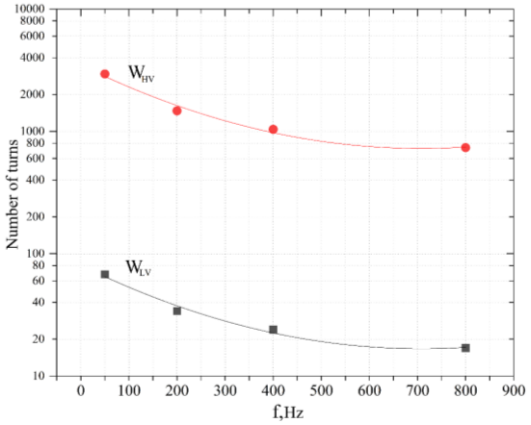

Fig. 7. *Dependence between the core remagnetization frequency and the number of turns of high voltage and low voltage windings*
Рис. 7. *Зависимость количества витков обмотки от частоты тока*

HTS transformer prototype

The presented paper considers a model of a HTS transformer with a spatial design (i.e. legs in different planes) of the magnetic system (Fig. 8). This design is characterized by the presence of the so-called "warm" magnetic core. It means that there is no direct contact between the core and the cryogenic medium. This technical solution imposes certain limitations on the design and production of the cryostat.

Table 2. *Technical parameters of the HTS transformer*
Таблица 2. *Технические параметры ВТСП трансформатора*

f (network frequency/частота сети), Hz	50	200	400	800
d (leg diameter/диаметр стержня), m	0.135	0.095	0.08	0.067
G_{st} (magnetic core weight/ масса магнитопровода), kg	432	184	123	81
E_t (turn EMF/ЭДС витка), V	3.382	6.701	9.623	13.32
w_{LV} (number of secondary turns/ количество витков вторичной обмотки)	68	34	24	17
w_{HV} (number of primary turns/ количество витков первичной обмотки)	2945	1473	1040	737
Φ_m (magnetic flow/магнитный поток), Wb	0.015	0.008	0.005	0.004
P_h (hysteresis losses/потери на гистерезис), W	171	297	396	532
P_{ed} (eddy current losses/потери на вихревые токи), W	25	223	594	1595
P_{id} (core losses/потери в сердечнике), W	196	521	990	2127

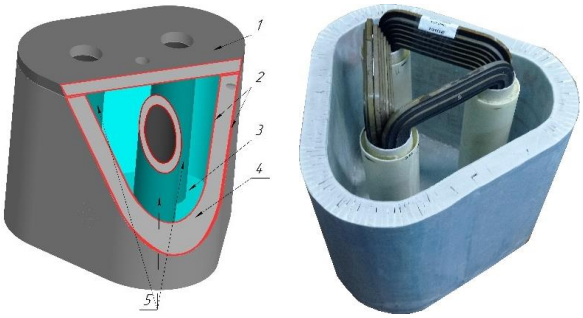

a *b*

Fig. 8. *HTS transformer design: a) 3D model of the cryostat with the spatial magnetic system: 1 – cryostat cover; 2 – glass fiber plastic; 3 – cryogenic medium with liquid nitrogen; 4 – polystyrene foam; 5 – thermal insulating tubes for magnetic core legs; b) prototype of a transformer*
Рис. 8. *Конструкция ВТСП трансформатора: а) 3D-модель кристалла с пространственной магнитной системой: 1 – крышка криостата; 2 – стеклотекстолит; 3 – криогенная среда с жидким азотом; 4 – пенополистирол; 5 – теплоизоляционные трубки для стержней магнитопровода; б) прототип трансформатора*

One of the key aspects of this design is the reduction of heat fluxes from the magnet core into the liquid nitrogen. Since the core is not directly located in the cryogenic circuit, heat losses caused by magnet core heating are minimized (Fig. 9). This will avoid losses of cryogenic liquid that has a positive effect on the transformer efficiency and diminishes the need for frequent replenishment of liquid nitrogen [28].

The simultaneous application of the spatial magnetic system (i.e. legs in different planes) allows reducing the core yoke size by half that considerably decreases the core weight. In this case, the full symmetry of the magnetic system is maintained. As a consequence, the no-load current of the transformer and the magnetic core losses are significantly reduced.

Fig. 9. *Industrial prototype of the HTS transformer*
Рис. 9. *Промышленный прототип ВТСП трансформатора*

Dielectric cryogenic medium in the form of liquid nitrogen

Liquid nitrogen is one of the most widely used cryogenic dielectrics. With a boiling temperature of 77 K, it has high thermal conductivity and low viscosity that makes it ideal for using in HTS cooling systems. Unlike many other dielectrics, polymers and some electrical oils, liquid nitrogen is not subject to aging processes that ensures the stability of its characteristics over time. Its simple molecular structure (N_2) eliminates the formation of decomposition products that also provides the reliability of systems using liquid nitrogen as a cooling agent [29].

The electrical breakdown in liquid nitrogen is possible in the presence of impurities, including unstable atoms, ions and insulation material deposits. These impurities can significantly reduce the electrical strength of the dielectric, so their presence should be strictly controlled. To prevent such problems, purification and filtration methods are used for nitrogen before using in critical applications. The physical properties of liquid nitrogen are summarized in Table 3.

Low reactivity helps to reduce or eliminate the liquid nitrogen impact on active (windings, magnetic core) and passive (insulating materials, cryostat) transformer elements.

Discussion of results

The conducted investigations confirmed the practicability of increasing the AC network frequency up to 800 Hz. This is especially important for considerable reduction of dimensional and weight parameters of electrical installations in mobile, autonomous and local power supply systems, as well as for solving geoengineering tasks when changing the location of geo-surveying works [30]

Table 3. *Physical properties of liquid nitrogen at 77.3 K and 0.10 MPa*

Таблица 3. *Физические свойства жидкого азота при температуре 77,3 К и 0,10 МПа*

Parameter Параметр	Value Величина
Molar mass, g·mol^{-1}/Молярная масса, г·моль$^{-1}$	28.01
Liquid phase density at saturation, kg·m^{-3} Плотность жидкой фазы при насыщении, кг·м$^{-3}$	807.4
Gas phase density at saturation, kg·m^{-3} Плотность газообразной фазы при насыщении, кг·м$^{-3}$	4604
Speed of sound in liquid phase, m·s^{-1} Относительная диэлектрическая проницаемость газообразного азота, м·с$^{-1}$	860
Volumetric expansion of liquid (77.3 K, 0.10 MPa) into gas (293 K, 0.10 MPa) Объемное расширение из жидкости (77.3 K, 0.10 МПа) в газ (293 K, 0.10 МПа)	1:694
Relative permittivity of liquid nitrogen Относительная диэлектрическая проницаемость жидкого азота	1.46
Relative permittivity of gaseous nitrogen Относительная диэлектрическая проницаемость газообразного азота	1.00
Electrical resistivity, Ohm·m Удельное электрическое сопротивление, Ом·м	>1·10^{16}
Surface tension, N·m^{-1} Поверхностное натяжение, Н·м$^{-1}$	8.9·10^{-3}
Dynamic viscosity, Pa·s/Динамическая вязкость, Па·с	1.65.10^{-4}
Thermal conductivity, W·m^{-1}·K^{-1} Теплопроводность, В·м$^{-1}$·К$^{-1}$	0.14
Heat capacity, J·g^{-1}·K^{-1}/Теплоемкость, Дж·г$^{-1}$·К$^{-1}$	2.04
Enthalpy of vaporization, J·g^{-1} Энтальпия парообразования, Дж·г$^{-1}$	199.3
Critical point at 3.35 MPa, K Критическая точка при 3,35 МПа, К	126.21
Triple point at 0.0125 MPa, K Тройная точка при 0,0125 МПа, К	63.1

In particular, in many power supply systems of this kind at river and sea vessels and aircrafts the transition to the higher frequency has already been performed. For example, 200 Hz frequency is used at hydrofoils in Russia, while 400 Hz frequency is used in the defense industry of some countries. However, having the possibility of reducing the resistance to zero in superconductors, it is reasonable to increase the frequency up to 800 Hz. This will allow achieving duplication of energy efficiency for electrical installations. In this case, energy efficiency is still estimated in considerable reduction of consumables or initial investments and decrease of active power losses during operation. Since energy efficiency is a system concept, it will be the subject of a separate paper. But it is quite obvious, since in remote power supply systems, for example, a geological expedition with variable location, the weight characteristics and dimensions are of great importance while moving. More important advantage is that the autonomous generation source used in such cases can have a smaller generation power, thus also reducing their cost. Finally, the replacement of the dielectric medium (i.e. liquid nitrogen) can be carried

out at any point of geolocation of the engineering team or expedition from the air using a turboexpander by the technology of Academician P. Kapitsa.

The paper demonstrates the frequency increase impact on the cross-section of winding conductors caused by the SE. In addition, it affects the magnetic core characteristics, that is why it is reasonable to use amorphous iron, and, in general, the mass and dimensions parameters of the transformer [31].

The obtained dependences, presented in Fig. 4, 6, 7, show that the synthesis of such parameters as the frequency increase and the amorphous iron magnetic core results in the exponential increase of heat losses in the magnetic core based on Steinmetz equations (11) and (12). This requires the decrease of the magnetic core induction with increasing electric current frequency that, in the end, affects the number of winding turns and the core weight. The presence of the cryostat requires 10–20 mm of wall thickness (Fig. 8) to maintain a cryogenic temperature of 77 K. This is generally compensated by the insulating layers between the windings and the magnetic core.

For example, the mass and dimensions parameters of a HTS transformer having the windings immersed in a cryostat, liquid nitrogen as a dielectric medium, and a warm magnetic core, are 432 kg at 50 Hz (industrial frequency), 123 kg at 400 Hz (i.e. 3.5 times less), and 86 kg at 800 Hz (i.e. more than 5 times less than at the industrial frequency).

It should be noted that a HTS transformer at the same frequency is more than 2–2.5 times smaller in dimensions than a conventional transformer [28, 32]. Taking into account the frequency increase, its mass and dimensions parameters are almost 10 times less than a conventional transformer at the industrial frequency. Therefore, it is more energy efficient than a conventional transformer by an order of magnitude [33–36].

In recent years, the tendency of increasing the operating frequency has become one of the main vectors of power industry development in distributed generation due to the improvement of technical and economic costs. In addition, the performance characteristics of sea and airborne transportation facilities are enhancing. However, this tendency is strongly limited by the phenomenon of current concentration near the conductor surface, the so-called SE, which increases the resistance of conductors and active power losses in them, thus reducing the energy efficiency of power equipment. For example, the resistance increases approximately 2.5–3 times at 400 Hz in comparison with the resistance at the industrial frequency of 50 Hz. As a consequence, active power losses in transformer windings increase proportionally to the resistance. While in the case of windings made of superconductor materials, it is reasonable to use the frequency of 800 and 1000 Hz. The use of HTS conductors in high frequency power equipment has a synergistic effect due to the fact that HTS is an absolute diamagnetic in the superconducting state that prevents the magnetic field penetration into the conductor depth and the formation of a surface layer.

The phenomenon of superconductivity and the possibility of ensuring it at the temperature of liquid nitrogen (77 K) opens almost unlimited directions for the use of higher frequencies, since the resistance is zero at any frequency, and, therefore, the problem of frequency limitation is completely eliminated. At present, this has not yet been realized by the power engineering community. In this paper, we have made an attempt to show that the mass and dimensions parameters of power equipment are reduced by 5–6 times at the frequency of 400 Hz applied for mobile systems when using superconducting windings, and by 9–12 times at the frequency of 800 Hz, which we reasonably suggest to investigate and implement.

An extremely important advantage of HTS transformers is the ability to self-limit short-circuit currents after leaving the superconducting state by a transformer, which is detailed in [32].

Conclusions

1. The practicability of the frequency increase up to 800 Hz instead of the industrial frequency of 50 Hz for mobile, autonomous and local power supply systems has been proved. In this case, active power losses in transformer windings are reduced to zero that allows increasing the current density from 2.4 to 500 A/mm^2 in HTS transformer windings. Then, it obviously results in the decrease of mass and dimensions parameters of HTS transformers and generation sources operated at the object.
2. It can be stated that the resistance of superconducting winding wires is reduced to zero when being of cryogenic design and in the dielectric medium in the form of liquid nitrogen (77 K). This results in removing the negative effect of forcing the current to the conductor surface with the frequency increase SE, in which the resistance increases by 2.5–3 times at 800 Hz. It is equivalent to the removal of the power consumer from the generation source at the distance of three times greater with the corresponding lengthening of the transmission line. However, this effect is not observed in superconductors, therefore it gives new opportunities for increasing the AC frequency.
3. In addition, it was shown that the use of amorphous iron as a core for a HTS transformer at higher frequencies reduces the magnetic core losses and increases the value of induction in the magnetic core.
4. The proposed technical solutions are implemented in the design and construction of the industrial prototype of 25 kVA, which confirmed the reliability of the general theoretical propositions on the energy efficiency.

REFERENCES

1. Arun P. Practical study of mixed-core high frequency power transformer. *Magnetism*, 2022, no. 2, pp. 306–327. DOI: 10.3390/2030022
2. Chan H. L., Cheng K.W.E., Sutanto D. Calculation of inductances of high frequency air-core transformers with superconductor windings for DC-DC converters. *IEE Proceedings: Electric Power Applications*, 2003, vol. 150, no. 4, pp. 447–454. DOI: doi.org/10.1049/ip-epa:20030257.
3. Liu G., Zhang G., Liu G., Wang H., Jing L. Experimental and numerical study of high frequency superconducting air-core transformer. *Superconducting Science Technology*, 2021, vol. 34, no. 8, Art. no. 85011.
4. Pronto A.G., Maurício A., Pina J.M. Magnetic properties measurement and discussion of an amorphous power transformer core at room and liquid nitrogen temperature. *Journal of Physics: Conference Series*, 2014, vol. 507, 032018. DOI: 10.1088/1742-6596/507/3/032018.
5. Arun P. Application prospects of hybrid magnetic circuits in high frequency power transformers. *Techrxiv*, 2022. DOI: 10.36227/techrxiv.21737858.v1
6. Yingying W., Xingyu Z., Xu C. Influence of saturation levels on transformer equivalent circuit model. *Electrical Engineering*, 2021, vol. 72, no. 6, pp. 381–387.
7. Yazdani-Asrami M., Gholamian S.A., Mirimani S.M. Influence of field-dependent critical current on harmonic AC loss analysis in HTS coils for superconducting transformers supplying non-linear loads. *Cryogenics*, 2021, vol. 113 (3), 103234. DOI: 10.1016/j.cryogenics.2020.103234
8. Grilli F., Ashworth S. Measuring transport AC losses in YBCO-coated conductor coils. *Superconductor Science and Technology*, 2007, vol. 20, pp. 794–799.
9. Lee S., Petrykin V., Molodyk A., Samoilenkov S., Kaul A., Vavilov A., Vysotsky V., Fetisov S. Development and production of second generation high Tc superconducting tapes at SuperOx and first tests of model cables. *Superconductor Science and Technology*, 2014, vol. 27, no. 4, Art. no. 044022.
10. Zhou J., Chan W., Schwartz J. Quench detection criteria for $YBa_2Cu_3O_7$-δ coils monitored via a distributed temperature sensor for 77 K cases. *IEEE Transactions on Applied Superconductivity*, 2018, vol. 28, no. 5, Art. no. 4703012.
11. Hu M., Zhou Q.B., Wang X., Tang F.P., Sheng J., Bian X.Y., Jin Z.J. Study of liquid nitrogen insulation characteristics for superconducting transformers. *IEEE Transactions on Applied Superconductivity*, 2022, vol. 32, no. 4, pp. 1–5, Art. no. 5500305.
12. Hellmann S., Abplanalp M., Elschner S., Kudymow A., Noe M. Current limitation experiments on a 1 mva-class superconducting current limiting transformer. *IEEE Transactions on Applied Superconductivity*, 2019, vol. 29, no. 5. DOI: 10.1109/TASC.2019.2906804.
13. Lei W., Jiaojiao W., Tian Y., Xiaoning H., Fushou X., Yanzhong L. Film boiling heat transfer prediction of liquid nitrogen from different geometry heaters. *International Journal of Multiphase Flow*, 2020, vol. 129, no. 103294.
14. Zabarilo D.A. Features of the calculation of a high-frequency power transformer. *Bulletin of the Dnepropetrovsk National. University of Railway Transport*, 2013, vol. 3 (45), pp. 29–35. (In Russ.)
15. Starodubtsev Yu.N. *Theory and calculation of a low-power transformer*. Moscow, IP Radiosoft Publ., 2017. 320 p. (In Russ.)
16. Tikhomirov P.M. *Calculation of transformers*. Moscow, Alliance Publ., 2009. 528 p. (In Russ.)
17. Malcolm S. R. Experimental measurements of the skin effect and internal inductance at low frequencies. *Article in Acta Technical CSAV (Ceskoslovensk Akademie Ved)*, 2015 vol. 60, pp. 51–69.
18. Coufal O. One hundred and fifty years of skin effect. *Applied Sciences*, 2023, vol. 13, no. 22. DOI: 10.3390/app132212416.
19. Corcoran J., Nagy P.B. Compensation of the skin effect in low-frequency potential drop measurements. *Journal of Nondestructive Evaluation*, 2016, vol. 35, no. 4. DOI: 10.1007/s10921-016-0374-4.
20. *ELCUT: modeling of electromagnetic, thermal and elastic fields by the finite element method. Version 6.6*. St. Petersburg, Publishing solutions Publ., 2023. 290 p. (In Russ.)
21. TS 14-123-215-2009 *magnetic tape pipelines made of soft magnetic amorphous alloys and soft magnetic composite material (nanocrystalline alloy)*. Asha, PJSC "Ashinsky Metallurgical Plant" Publ., 2011. 15 p. (In Russ.)
22. Lenke R.U., Rohde S., Mura F., De Doncker R.W. Characterization of amorphous iron distribution transformer core for use in high-power medium-frequency applications. *IEEE Energy Conversion Congress and Exposition*. San Jose, CA, USA, 2009. DOI: 10.1109/ECCE.2009.5316134.
23. Kurita N., Nishimizu A., Kobayashi C., Tanaka Y., Yamagishi A., Ogi M. Magnetic properties of simultaneously excited amorphous and silicon steel hybrid cores for higher efficiency distribution transformers. *IEEE Transactions on Magnetics*, 2018, vol. 54, no. 11. DOI: 10.1109/TMAG.2018.2835498.
24. Elgamli E., Anayi F. Advancements in electrical steels: a comprehensive review of microstructure, loss analysis, magnetic properties, alloying elements, and the influence of coatings. *Applied Sciences*, 2023, vol. 13, no. 18. p. 10283. DOI: 10.3390/app131810283.
25. Azuma D., Ito N., Ohta M. Recent progress in Fe-based amorphous and nanocrystalline soft magnetic materials. *Journal of magnetism and magnetic materials*, 2020, vol. 501. DOI: https://doi.org/10.1016/j.jmmm.2019.166373
26. Suzuki K., Fujimori H., Hashimoto K. *Amorphous metals.* Ed. by Ts. Masumoto. Translated from Japanese. Japan, Metallurgy Publ., 1987. 328 p.
27. Pejush C.S., Youguang G., Hai Y.L., Jian G.Z. Measurement modelling of rotational core loss of fe-based amorphous magnetic material under 2-d magnetic excitation. *IEEE Transactions on Magnetics*, 2021, pp. (99):1-1. DOI: 10.1109/TMAG.2021.3111498
28. Manusov V.Z., Galeev R.G. Estimation of parameters of a superconducting hybrid transformer with a spatial magnetic system. *Electricity*, 2024, no. 12, pp. 15–26. (In Russ.) DOI: 10.24160/0013-5380-2024-12-15-26.
29. Kang J., Lee H., Kang H. Dielectric Characteristics of liquid nitrogen according to the electrode material. *Journal of Superconductivity and Novel Magnetism*, 2015, no. 28 (3), pp. 1167–1173. DOI: 10.1007/s10948-014-2677-y.
30. Obukhov S.G., Beloglazkin A.O. Engineering methodology for designing power supply systems for autonomous energy-efficient buildings based on renewable energy sources. *Bulletin of the Tomsk Polytechnic University. Geo Assets Engineering*, 2023. vol. 334, no. 1, pp. 30–42. (In Russ.) DOI: 10.18799/24131830/2023/1/3900

31. Ibrahim M., Pillay P. Core loss prediction in electrical machine laminations considering skin effect and minor hysteresis loops. *IEEE Transactions on Industry Applications*, 2013, vol. 49, no. 5, pp. 2061–2068. DOI: 10.1109/TIA.2013.2260852.
32. Jaroszynski L., Wojtasiewicz G., Janowski T. Considerations of 2G HTS Transformer Temperature During Short Circuit. *IEEE Transactions on Applied Superconductivity*, 2018, vol. 28, no. 4. DOI: 10.1109/TASC.2018.2806561.
33. Sarker P.C., Md. Islam R., Guo Y., Zhu J., Lu H.Y. State of art technologies for development of high frequency transformers with advanced magnetic materials. *IEEE Transactions on Applied Superconductivity*, 2019, vol. 29, no. 2. DOI: 10.1109/TASC.2018.2882411.
34. Oliveira S.V.G., Barbi I. A three-phase step-up DC-DC converter with a three-phase high frequency transformer. *Proceedings of the IEEE International Symposium on Industrial Electronics*, 2005. DOI: 10.1109/ISIE.2005.1528980.
35. Nanato N., Adachi T., Yamanishi T. Development of single-phase bi2223 high temperature superconducting transformer with protection system for high frequency and large current source. *Journal of Physics*: *Conference Series*, *vol. 1293. 31st International Symposium on Superconductivity (ISS2018)*. Tsukuba, Ibaraki, Japan, 12–14 December 2018. DOI: 10.1088/1742-6596/1293/1/012072.
36. Kondratowicz-Kucewicz B., Wojtasiewicz G. The proposal of a transformer model with winding made of parallel 2g HTS tapes with transpositioners and its contact cooling system. *IEEE Transactions Applied Superconductivity*, 2018, vol. 28, no. 4. DOI: 10.1109/TASC.2018.2807585.

Information about the authors
Ratmir G. Galeev, Assistant, Novosibirsk State Technical University, 20, Karl Marx avenue, Novosibirsk, 630073, Russian Federation. galeew.ratmir@yandex.ru orcid.org/0009-0004-0485-6786
Vadim Z. Manusov, Dr. Sc., Professor, Yugra State University, 16, Chekhov street, Khanty-Mansiysk, 628011, Russian Federation. manusov36@mail.ru orcid.org/0000-0001-7799-4830
Evgeny N. Larkin, Postgraduate Student, Siberian State University of Water Transport, 33, Shchetinkin street, Novosibirsk, 630099, Russian Federation. hade876@yandex.ru

Received: 08.10.2024
Revised: 14.11.2024
Accepted: 24.01.2025

СПИСОК ЛИТЕРАТУРЫ

1. Arun P. Practical study of mixed-core high frequency power transformer // Magnetism. – 2022. – № 2. – P. 306–327. DOI: 10.3390/2030022
2. Chan H.L., Cheng K.W.E., Sutanto D. Calculation of inductances of high frequency air-core transformers with superconductor windings for DC-DC converters // IEE Proceedings: Electric Power Applications. – 2003. – Vol. 150. – № 4. – P. 447–454. DOI: doi.org/10.1049/ip-epa:20030257.
3. Experimental and numerical study of high frequency superconducting air-core transformer / G. Liu, G. Zhang, G. Liu, H. Wang, L. Jing // Superconducting Science Technology. – 2021. – Vol. 34. – № 8. – Art. no. 85011.
4. Pronto A.G., Maurício A., Pina J.M. Magnetic properties measurement and discussion of an amorphous power transformer core at room and liquid nitrogen temperature // Journal of Physics: Conference Series. – 2014. – Vol. 507. – 032018. DOI: 10.1088/1742-6596/507/3/032018.
5. Arun P. Application prospects of hybrid magnetic circuits in high frequency power transformers // Techrxiv. – 2022. DOI: 10.36227/techrxiv.21737858.v1
6. Yingying W., Xingyu Z., Xu C. Influence of saturation levels on transformer equivalent circuit model // Electrical Engineering. – 2021. – Vol. 72. – № 6. – P. 381–387.
7. Yazdani-Asrami M., Gholamian S.A., Mirimani S.M. Influence of field-dependent critical current on harmonic AC loss analysis in HTS coils for superconducting transformers supplying non-linear loads // Cryogenics. – 2021. – Vol. 113 (3). – 103234. DOI: 10.1016/j.cryogenics.2020.103234
8. Grilli F., Ashworth S. Measuring transport AC losses in YBCO-coated conductor coils // Superconductor Science and Technology. – 2007. – Vol. 20. – P. 794–799.
9. Development and production of second generation high Tc superconducting tapes at SuperOx and first tests of model cables / S. Lee, V. Petrykin, A. Molodyk, S. Samoilenkov, A. Kaul, A. Vavilov, V. Vysotsky, S. Fetisov // Superconductor Science and Technology. – 2014. – Vol. 27. – № 4. – Art. no. 044022.
10. Zhou J., Chan W., Schwartz J. Quench detection criteria for YBa2Cu3O7-δ coils monitored via a distributed temperature sensor for 77 K cases // IEEE Transactions on Applied Superconductivity. – 2018. – Vol. 28. – № 5. – Art. no. 4703012.
11. Study of liquid nitrogen insulation characteristics for superconducting transformers / M. Hu, Q.B. Zhou, X. Wang, F.P. Tang, J. Sheng, X.Y. Bian, Z.J. Jin // IEEE Transactions on Applied Superconductivity. – 2022. – Vol. 32. – № 4. – P. 1–5. – Art. no. 5500305.
12. Current limitation experiments on a 1 mva-class superconducting current limiting transformer / H S. Ellmann, M. Abplanalp, S. Elschner, A. Kudymow, M. Noe // IEEE Transactions on Applied Superconductivity. – 2019. – Vol. 29. – № 5. DOI: 10.1109/TASC.2019.2906804.
13. Film boiling heat transfer prediction of liquid nitrogen from different geometry heaters / W. Lei, W. Jiaojiao, Y. Tian, H. Xiaoning, X. Fushou, L. Yanzhong // International Journal of Multiphase Flow. – 2020. – Vol. 129. – № 103294.
14. Забарило Д.А. Особенности расчета силового трансформатора повышенной частоты // Наука та прогресс транспорту. – 2013. – № 3 (45). – С. 29–35.
15. Стародубцев Ю.Н. Теория и расчет трансформаторов малой мощности. – М.: ИП Радиософт, 2017. – 320 с.
16. Тихомиров П.М. Расчет трансформаторов. – М.: М. Альянс, 2009. – 528 с.

17. Malcolm S.R. Experimental measurements of the skin effect and internal inductance at low frequencies // Article in Acta Technical CSAV (Ceskoslovensk Akademie Ved). – 2015. – Vol. 60. – P. 51–69.
18. Coufal O. One hundred and fifty years of skin effect // Applied Sciences. – 2023. – Vol. 13. – № 22. DOI: 10.3390/app132212416.
19. Corcoran J., Nagy P.B. Compensation of the skin effect in low-frequency potential drop measurements // Journal of Nondestructive Evaluation. – 2016. – Vol. 35. – № 4. DOI: 10.1007/s10921-016-0374-4.
20. ELCUT: Моделирование электромагнитных, тепловых и упругих полей методом конечных элементов. Версия 6.6. Руководство пользователя. – Издательские решения, 2023. – 290 с.
21. ТУ 14-123-215-2009 Магнитопроводы ленточные из магнитомягких аморфных сплавов и магнитомягкого компазиционного материала (нанокристаллического сплава). – Аша: ПАО «Ашинский металургическиз завод», 2011. – 15 с.
22. Characterization of amorphous iron distribution transformer core for use in high-power medium-frequency applications / R.U. Lenke, S. Rohde, F. Mura, R.W. de Doncker // IEEE Energy Conversion Congress and Exposition. – San Jose, CA, USA, 2009. DOI: 10.1109/ECCE.2009.5316134.
23. Magnetic properties of simultaneously excited amorphous and silicon steel hybrid cores for higher efficiency distribution transformers / N. Kurita, A. Nishimizu, C. Kobayashi, Y. Tanaka, A. Yamagishi, M. Ogi // IEEE Transactions on Magnetics. – 2018. – Vol. 54. – № 11. DOI: 10.1109/TMAG.2018.2835498.
24. Elgamli E., Anayi F. Advancements in electrical steels: a comprehensive review of microstructure, loss analysis, magnetic properties, alloying elements, and the influence of coatings // Applied Sciences. – 2023. – Vol. 13. – № 18. – P. 10283. DOI: 10.3390/app131810283.
25. Azuma D., Ito N., Ohta M. Recent progress in Fe-based amorphous and nanocrystalline soft magnetic materials // Journal of magnetism and magnetic materials. – 2020. – Vol. 501. DOI: https://doi.org/10.1016/j.jmmm.2019.166373
26. Suzuki K., Fujimori H., Hashimoto K. Amorphous metals / Ed. by Ts. Masumoto Translated from Japanese. – Japan: Metallurgy Publ., 1987. – 328 p.
27. Measurement modelling of rotational core loss of fe-based amorphous magnetic material under 2-d magnetic excitation / C.S. Pejush, G. Youguang, Y.L. Hai, G.Z. Jian // IEEE Transactions on Magnetics. – 2021. – P. (99):1-1. DOI: 10.1109/TMAG.2021.3111498
28. Минусов В.З. Галеев Р.Г. Оценка параметров сверхпроводящего гибридного трансформатора с пространственной магнитной системой // Электричество. – 2024. – № 12. – С. 15–26. DOI: 10.24160/0013-5380-2024-12-15-26.
29. Kang J., Lee H., Kang H. Dielectric characteristics of liquid nitrogen according to the electrode material // Journal of Superconductivity and Novel Magnetism. – 2015. – № 28 (3). – P. 1167–1173. DOI: 10.1007/s10948-014-2677-y.
30. Обухов С.Г., Давыдов Д.Ю., Белоглазкин А.О. Инженерная методика проектирования систем электроснабжения автономных энергоэффективных зданийна основе возобновляемых источников энергии // Известия Томского политехнического университета. Инжиниринг георесурсов. – 2023. – Т. 334. – № 1. – С. 30–42. DOI: 10.18799/24131830/2023/1/3900.
31. Ibrahim M., Pillay P. Core loss prediction in electrical machine laminations considering skin effect and minor hysteresis loops // IEEE Transactions on Industry Applications. – 2013. – Vol. 49. – № 5. – P. 2061–2068. DOI: 10.1109/TIA.2013.2260852.
32. Jaroszynski L., Wojtasiewicz G., Janowski T. Considerations of 2G HTS transformer temperature during short circuit // IEEE Transactions on Applied Superconductivity. – 2018. – Vol. 28. – № 4. DOI: 10.1109/TASC.2018.2806561.
33. State of art technologies for development of high frequency transformers with advanced magnetic materials / P.C. Sarker, Md.R. Islam, Y. Guo, J. Zhu, H.Y. Lu // IEEE Transactions on Applied Superconductivity. – 2019. – Vol. 29. – № 2. DOI: 10.1109/TASC.2018.2882411.
34. Oliveira S.V.G., Barbi I. A three-phase step-up DC-DC converter with a three-phase high frequency transformer // Proceedings of the IEEE International Symposium on Industrial Electronics. – 2005. DOI: 10.1109/ISIE.2005.1528980.
35. Nanato N., Adachi T., Yamanishi T. Development of single-phase bi2223 high temperature superconducting transformer with protection system for high frequency and large current source // Journal of Physics: Conference Series. Vol. 1293. 31st International Symposium on Superconductivity (ISS2018). – Tsukuba, Ibaraki, Japan, 12–14, 2018. DOI: 10.1088/1742-6596/1293/1/012072.
36. Kondratowicz-Kucewicz B., Wojtasiewicz G. The proposal of a transformer model with winding made of parallel 2g HTS tapes with transpositioners and its contact cooling system // IEEE Transactions Applied Superconductivity. – 2018. – Vol. 28. – № 4. DOI: 10.1109/TASC.2018.2807585.

Информация об авторах

Ратмир Гаязович Галеев, ассистент кафедры теоретических основ электротехники, Новосибирский государственный технический университет, Россия, 630073, г. Новосибирск, пр. Карла Маркса, 20. galeew.ratmir@yandex.ru orcid.org/0009-0004-0485-6786

Вадим Зиновьевич Манусов, доктор технических наук, профессор, профессор физико-математической школы, Югорский государственный университет, Россия, 628011, г. Ханты-Мансийск, ул. Чехова, 16. manusov36@mail.ru

Евгений Николаевич Ларкин, аспирант кафедры электрооборудования и автоматики, Сибирский государственный университет водного транспорта, Россия, 630099, г. Новосибирск, ул. Щетинкина, 33. shade876@yandex.ru

Поступила в редакцию: 08.10.2024
Поступила после рецензирования: 14.11.2024
Принята к публикации: 24.01.2025